

IMECE2012-87736

## SMALL WIND TURBINE TOWER STRUCTURAL VIBRATION

Ehsan Mollasalehi, David H. Wood, Qiao Sun

Department of Mechanical Engineering  
Schulich School of Engineering  
University of Calgary  
Calgary, AB, Canada  
Email: emollasa | dhwood | qsun @ucalgary.ca

### ABSTRACT

A major barrier to the acceptance of small wind turbines is that they are perceived to be noisy particularly when mounted on monopole towers rather than traditional guy-wired ones. This paper discusses an aspect of noise propagation that has not been studied previously: vibration of the tower. To start studying the tower's behavior, twenty four accelerometers were attached in two orthogonal lines along the 10 m tower of Southwest Windpower Skystream 2.4 kW wind turbine located at the edge of the city of Calgary. About 15 minutes of data were recorded in order to extract natural frequencies and corresponding mode shapes while the turbine was in operating. Operational modal analysis (OMA), in which input loads are considered the ambient input, is conducted to identify dominant modes up to 100 Hz. This range covers the infrasound region (<20 Hz) that might be perceived at sufficiently high sound pressure levels. The captured modal frequencies and modal shapes compared favorably to those predicted by a finite element analysis. Results indicate that a cluster of modes located around 10 Hz show significantly higher magnitude than other modes. This corresponds to the second bending mode. Short-time Fourier transform was used to distinguish natural and forced frequencies. It was seen that higher modes were excited less than lower ones. Original signals were decomposed using discrete wavelet transform to obtain different frequency bands. Relative root mean square values for each frequency band were calculated to determine the contribution to the vibration energy. It was observed that most of vibration energy occurs in the lowest frequency band which is in the infrasound region. The accelerometers were monitored while the blades and generator accelerated and decelerated as the wind speed

changed, and only the first bending mode was excited significantly which apparently generates most of noise emission.

*Keywords: small wind turbine, wind turbine noise, tower vibration, noise propagation, operational modal analysis, discrete wavelet transform*

### INTRODUCTION

Wind turbines generally produce sound both mechanically and aerodynamically. Although modern wind turbines are quiet, noise propagation is still an important issue. Noise emissions from large wind turbines have been one of the more studied areas in wind energy engineering [1]. On the other hand, there are not many studies of the noise from small wind turbines (SWT) in the literature [2]. SWTs are often located in the owner's yard. Thus, neighborhood reactions to small turbine noise may be important. Sources of wind turbine noise have been classified mainly into four categories: tonal, broadband, low frequency and infrasound, and impulsive [3]. Tonal noise is caused by wind turbine components such as gear meshing which is most common in large turbines. Small turbines studied in this paper typically do not have a gearbox. Broadband noise has frequency components higher than 100 Hz caused mainly by the interaction of blades with the atmospheric turbulence, leading to "swishing". Infrasound refers to frequencies below the hearing threshold: 20 Hz. The low frequency range between 20 and 100 Hz is suspected of being irritating for many people, and includes contributions from blade-tower noise for downwind rotors. Impulsive noise is described by short acoustic impulses. Infrasound and low frequency noise, which

are the authors' interest, can be amplified and radiated by tower structure. Tower vibrations are likely to come from vibrations in the generator and once-per-revolution feeding from the blades to the main shaft as well as any eccentricities in the generator rotor etc. Even if the tower sound power level is small, the tower approximates a line source and also may act as an amplifier. Therefore, noise will be attenuated less rapidly than the "point source" aerodynamic noise from the rotor. In addition, small turbines are often placed much closer to houses than large ones.

Because of their small power outputs, it is often difficult to accurately measure small wind turbine noise in order to derive meaningful conclusions. Instead, in this paper, tower vibration is studied to provide the basis to investigate the acoustic propagation.

Marmo and Carruthers et al. [4] studied aspects of structural vibration of a large turbine tower. They showed that vibrations caused by gear tooth meshing were transmitted through the gearbox isolators and finally into the tower structure. These vibrations then could be amplified by tower before propagating as problematic tonal noise. To reduce these noises, they suggested different amounts of damping laminate be applied to the inside of the tower adjacent to the nacelle, which affects sound level outside the tower. As far as the authors are aware there are no other detailed studies of wind turbine tower vibration in connection with noise.

Vibration analysis can be done by performing Operational Modal Analysis (OMA), also called Output-only Modal Analysis. This is a relatively a new approach compared to experimental modal analysis, where structural parameters are calculated only from response data assuming the input force is ambient [5,6]. This technique has been applied for more than a decade on civil structures such as towers where artificial excitation is a problem or estimation of actual excitation such as wind is very difficult. There are several techniques to estimate modal parameters from only response data. They include, for instance, peak-picking from power spectral density (PSD) [7], autoregressive moving average (ARMA) [8], and natural excitation technique (NExT) [9]. Among different methods, the Frequency Domain Decomposition (FDD) is applied to capture resonant frequencies and corresponding mode shapes based on auto/cross spectral densities between different channels. It uses cross-power spectral density instead of frequency response function and auto/cross correlations instead of impulse response function to determine the parameters from output data.

Since frequency components may vary during data acquisition because of different input loads, frequency domain and time domain characteristics should be related in order to find out how and when these dominant components arise. To observe dominant components as operating conditions vary, one may use Short-time Fourier Transform (STFT) which provides frequency information at discrete times. The STFT breaks down a non-stationary time series into many small pieces, which can be supposed to be locally stationary, and then applies the conventional FFT to these segments. Results, are

often presented in a 3D plot in which at each specific time, the excited frequency magnitudes are shown.

Investigation on tower's behavior can go further by observing vibration energy distribution. Since the signal's energy is proportional to the sum of the squares of its magnitudes, survey on energy distribution among different frequency bands can be done by using relative Root Mean Square (RMS) values. Discrete wavelet transforms may be used in order to decompose the time series with different frequency resolutions; using a larger time window for lower frequencies and smaller ones for higher frequencies.

The following section presents the experiment setup followed by an overview of frequency-domain OMA. This includes STFT results and related discussions. At the end, energy distribution using discrete wavelet transform will be brought.

## MEASUREMENT SETUP

The test was performed on the 10.2 m tower of a 2.4 kW wind turbine with downwind rotor with stall-regulation control. The turbine's control system implements a maximum power tracking strategy that aims to make the generator frequency as close as possible to a constant factor times the wind speed. The rotor diameter and swept area was 3.72m, and is shown in fig. 1 and fig. 2. The tower is a one-piece monopole with a base diameter of 0.2756 m and a top diameter of 0.1567 m and thickness 3.416 mm. The turbine is allowed to yaw freely with yaw stability provided by the downwind deflection of the blades.



Figure 1: Skystream wind turbine having accelerometers fixed

Twenty four accelerometers were attached along two orthogonal lines to the tower, made of S105 steel. The tower was lowered and raised using the gin pole and truck seen in the centre of fig. 1 and was bolted to the foundations as for a normal installation for the duration of these experiments. Fortunately data was successfully gathered from all 24 accelerometers. The single-axis B&K 4508-B piezoelectric accelerometers were arranged equally along the length of the

tower, approximately 90cm apart. This type of accelerometer can be used in a wide range of temperature with frequency range of 0.3 – 8000 Hz, and sensitivity of 100 mV/g. The data acquisition module was a portable NI9234 with a sampling rate of 2.5 kHz. In this work, the time series was down-sampled at a rate of 200 Hz so that signal contents up to 100 Hz are reliably maintained. Several data collections were done over periods of 15 to 30 minutes to capture low frequencies. The reference channel was chosen to be the most bottom one since it has the least vibration.

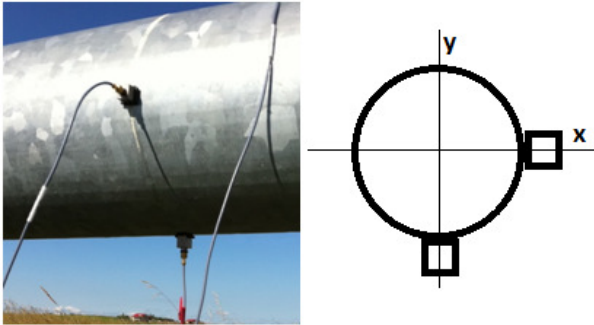


Figure 2: Accelerometers on two orthogonal axes

Generally, points that are nodal points are good options to be reference. As a sample, the raw data for channel 12 which is at the top of the tower is shown in fig. 3. Most of the measurements were done in order to only apply vibration analysis; however, the last one was synchronized to a wireless module which can connect to the antenna at the top of the turbine to measure the rotor angular velocity and output power.

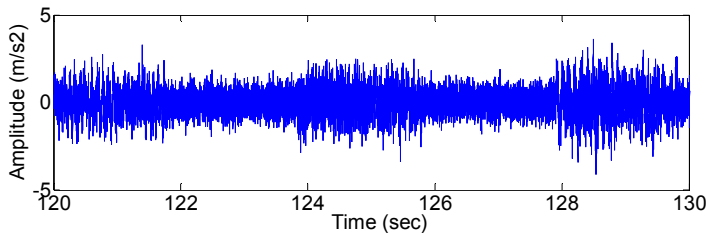


Figure 3: 10 second of raw data for top sensor

During the measurement, the SWT reached a maximum output power of about 460 W as is shown in fig. 4. Most fluctuations in power generation and angular velocity occur almost at the end of the measurement. In fact, RPM and power generation logs follow a same trend as required for optimum power extraction. At the very beginning of data acquisition, blades reached to the maximum speed of about 150 RPM and the output power reached 55 W. In the middle of data collection, there was no wind and consequently no power generation. However, the wind picked up for the final section of log and as a result, the SWT reached about 460 W.

This SWT begins generating power in a wind approximately 3.5m/s. At this speed the blades rotate at around 120 rpm. Once it has started producing power, it continues to produce power at lower speeds down to about 80 rpm.

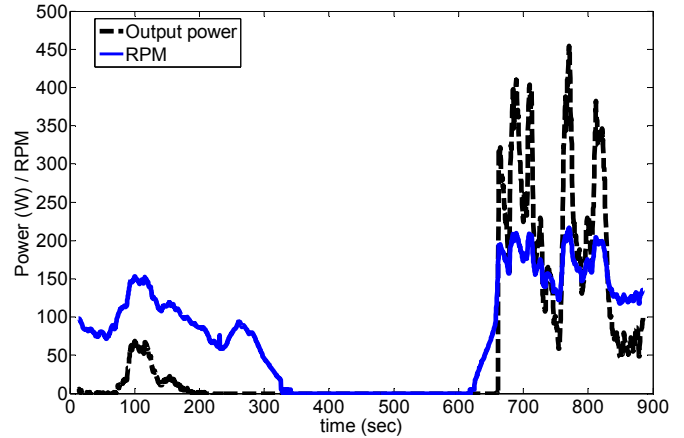


Figure 4: Blades rotational speed and power logs

### OPERATIONAL MODAL ANALYSIS

Modal analysis is a method to determine modal parameters of a system. This system may be defined as a simple structure or a more complex system including several subsystems. The modal parameters that completely describe the dynamics of a system are: modal frequency, modal damping, and mode shape. Any forced dynamic deflection of a structure can be represented as a weighted sum of its mode shapes. Each mode is considered a degree of freedom. A general modal test of a system is performed by measuring the input force and output responses with some assumptions, such as linearity and time-invariance. The excitation is either transient or random. An alternative modal analysis approach is called operational modal analysis by which the system parameters are calculated by advanced signal processing tools by only measuring the response of the structure. This technique has been used successfully in buildings, bridges, platforms, and towers where the natural excitation of wind extracts the parameters such as [10].

The advantage of this approach is that the modal parameters can be extracted while the structure is operating implying real boundary conditions and vibration levels. The other benefit is that the test component does not need to be isolated from the structure. For instance, in our application, to calculate parameters for the tower, one can perform the test without detaching the blades from the tower. The measurement procedure is similar to operational deflection shape measurement where one channel is considered as a reference for the output of the accelerometers for the response for all degrees of freedom. The inputs to the system are assumed to be zero mean Gaussian white signals. In this investigation, input forces come from wind load and vibration transmitted from the generator and rotor imbalance, and blades thrust.

Frequency Domain Decomposition (FDD) is an extension of the usual frequency domain method. FDD uses singular value decomposition for each frequency line to extract modal parameters. Input force and output response have the following relationship:

$$[G_y(j\omega)] = [H(j\omega)]^* [G_x(j\omega)] [H(j\omega)]^T \quad (1)$$

where  $G_x(j\omega)$  and  $G_y(j\omega)$  are the input and output power spectral density (PSD) matrices, respectively.  $H(j\omega)$  is Frequency Response Function (FRF) of the tower. With the assumption of zero mean and white,  $G_x$  is constant. The FRF matrix can be written in the form of [11,12]:

$$[H(j\omega)] = \sum_{k=1}^m \frac{[R_k]}{j\omega - \lambda_k} + \frac{[R_k]^*}{j\omega - \lambda_k^*} \quad (2)$$

where  $m$  is the number of modes,  $\lambda_k$  is the eigenfrequency for the  $k$ th mode.  $[R_k]$  is residue matrix consisting of mode shape and modal participation vector which describes relatively how well a particular mode is excited. Combining eqs. (1), and (2) the structural response can be expressed in terms of modal properties as:

$$[G_y(j\omega)] = \sum_{k \in \text{Sub}(\omega)} \frac{d_k \psi_k \psi_k^H}{j\omega - \lambda_k} + \frac{d_k^* \psi_k^* \psi_k^H}{j\omega - \lambda_k^*} \quad (3)$$

where  $d$  is a scalar constant,  $\psi$  is the modal participation, and  $\text{Sub}(\omega)$  is the set of modes that contribute at the specific frequency. In a word, cross-power spectral density instead of FRF and auto-correlation instead of impulse response function are used in eq. (1) to achieve eq. (3).

To start the analysis, Fast Fourier Transforms (FFT) were performed on the raw time series data from all accelerometers to compute spectral densities after using the low and high pass filters to remove unwanted components. A windowing function should be used to minimize leakage and noise, such as Hanning or Hamming. In this study, the Periodic Hamming window was used following removing the mean value. Then, the spectral density matrices are calculated for every series of measurements which gives us a series of matrices of size  $n \times n$  where  $n$  is number of accelerometers. In our case  $n=12$ , then the typical matrix would be:

$$G(j\omega) = \begin{bmatrix} PSD_{1,1}(j\omega) & CSD_{1,2}(j\omega) & \dots & CSD_{1,12}(j\omega) \\ CSD_{21}(j\omega) & PSD_{2,2}(j\omega) & \dots & CSD_{2,12}(j\omega) \\ \vdots & \vdots & \ddots & \vdots \\ CSD_{12,1}(j\omega) & CSD_{12,2}(j\omega) & \dots & PSD_{12,12}(j\omega) \end{bmatrix} \quad (4)$$

where  $G$  is cross-correlation function, and the diagonal elements of the matrix represent the magnitude of the spectral densities for each channel, i.e. power spectral density (PSD), and off-diagonal terms are the cross spectral densities (CSDs) between each channel and other responses.  $CSD_{pq}(j\omega) = CSD_{qp}^*(j\omega)$  as the matrix is Hermitian.  $PSDs$  are real valued while  $CSDs$  have phase information between the measurement and reference point.

One can decompose the last matrix into singular values and singular vectors by applying Singular Value Decomposition (SVD), generally, as

$$A = U S V^H \quad (5)$$

where  $S$  contains singular values, and  $U$  and  $V$  are unitary matrices. This technique is applied for each frequencies and measurements. The explained technique can be applied on different section of the collected data, for example, when wind is blowing or not with different defined overlaps.

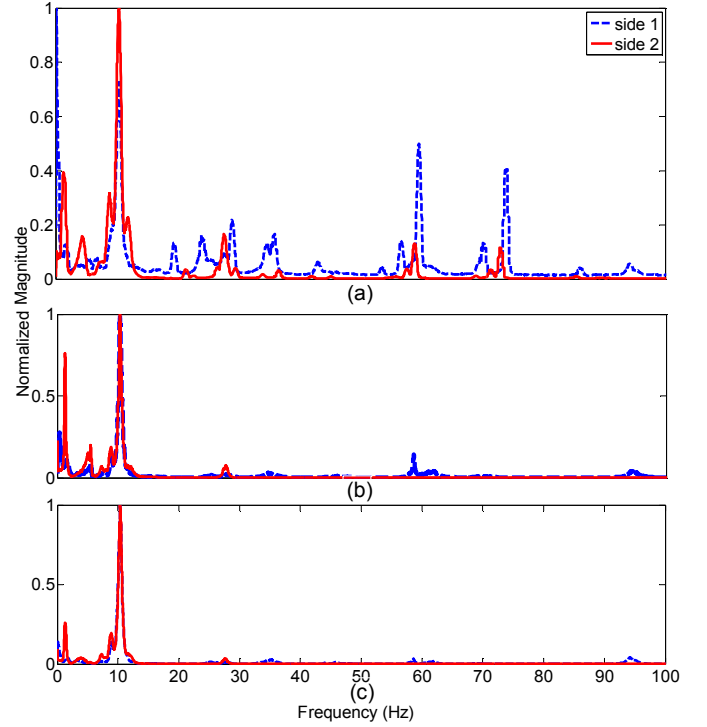


**Figure 5: Frequency response; a) entire data b) first- c) second- 2/3 of data at middle of collected data. The x-scale is the same for all three parts of the figure.**

Concurrently, a Finite Element Model was built in order to compare measured frequencies with computer model. The tower geometry was defined based on manufacturer's technical specifications. The turbine was represented by its mass attached to the tower with its center of mass 400mm downwind of the tower. To start applying modal analysis, certain loading conditions on the tower were added to simulate certain forces such as wind shear, thrust force caused by the turbine and the moment caused by the overhanging mass and gyroscopic moment. The much smaller moment arising in reaction to the generator torque was ignored. However the additional forces had little effect of the modal frequencies or mode shapes as the natural frequencies of the tower are independent of the forcing function. Table 1 includes natural frequencies from this model.

Figure 5(a) represents frequency decomposition for the orthogonal sides for the entire measurement. Side 1 data in blue shows the response for accelerometers on X axis, while the red side 2 line shows Y axis response. The noticeable peaks are listed in Table 1 in the company of FEM determination of the

natural frequencies. Note that S1 and S2 stand for Side 1 and Side 2 respectively.

Table 1 shows that most of natural frequencies were excited but there are some other frequencies among them which are suspected to be forced components. To determine which frequencies were excited while the blades were not spinning the middle section of the data in fig. 4 was excised (300 to 600 sec). This section was divided in two halves with 33% overlap. Frequency responses were then determined, fig. 5(b) and fig. 5(c). Although there were small peaks at higher frequencies, it seems that wind itself did not excite all natural modes. First mode (1.3 Hz), and second mode (10.4 Hz), on the other hand, resonated easily.

No	S1	S2	FEM S1	FEM S2	No	S1	S2	FEM S1	FEM S2
1	0.15	0.16			11	34.6	33.8		
2		1.33	1.33	1.332	12	35.9	36.7		
3		4.48			13	43.1	45.2	42.0	
4		8.82			14	56.6			
5	10.4	10.3	9.52	9.71	15	59.7	58.8		60.2
6		11.9			16	70.3	72.9	69.0	
7	19.5	21.3		19.93	17	73.8			
8	23.9		24.3		18	85.9	85.4		
9	28.9	27.5			19	94.2		99.7	
10		29.5		31.04					

Table 1: Dominant frequencies according to fig. 5 and FEM

ODS is generally the deflection of a structure at a specific frequency. This deflection is the motion of one point relative to others. It is a vector meaning that includes location and direction. It contains the values of a set of frequency domain responses at a particular frequency. Since ODS is a relative motion, it requires a fixed reference point which was chosen the bottommost accelerometer, because this point has the least vibration. Figure 6 displays some of the important ODSs. (*X*) and (*Y*) stand for *X*- and *Y*-directions.

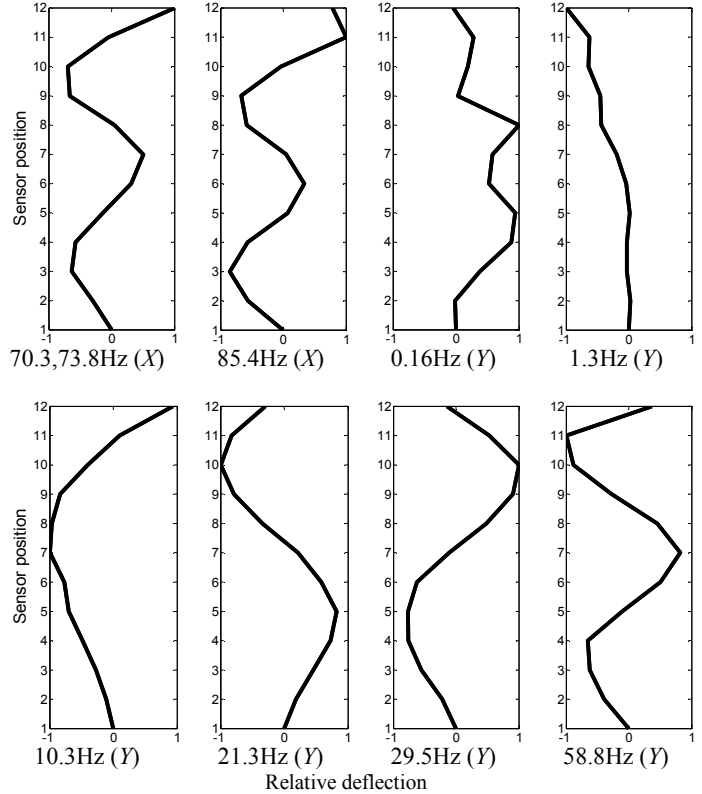
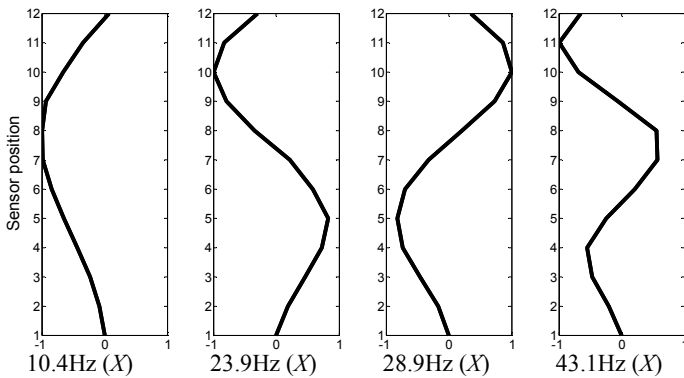


Figure 6: Operational deflection shapes

It is important to note that these deformations are not actual mode shapes meaning they are not scaled by the input force and consequently would not supply scaled shapes. These ODSs represent normalized mode shapes with the familiar shape of the first and other modes of a horizontal cantilever beam. The first frequency from table 1 is 0.15 Hz which does not agree with the FEM, i.e. 1.4 Hz, and its deflection shape does not follow the typical first mode. So, it is assumed to be unwanted component. First mode in *X* direction was not captured; however, in the *Y* direction shows the first bending mode. FEM indicates that there should be a resonance frequency at about 69 Hz. However, the measured peaks at 70.3 and 73.8 Hz, which are the closest peaks from to 69 Hz fig. 5, have exactly the same ODS, so, each of them can act as fifth mode. 21.3 Hz shows the same deflection as 29.5 Hz, but in opposite direction. This frequency, according to FEM, has a combination motion including both bending and torsion.

### Short-time Fourier Transform

In the previous analyses, it was assumed that wind and other input loads are stationary, yet it is time-varying. Thus, it would force some local unwanted frequencies to the system. To investigate the time dependence further, Short-Time Fourier Transform (STFT) was used to analyze much shorter data sequences. This allows assessment of how the important frequencies vary and how they relate to the turbine power and blade speed. Briefly, the time series is decomposed into several

short periods of time, and FFT applied. Mathematically, the process can be written as

$$X(m, \omega) = \sum_{n=-\infty}^{\infty} x[n] w[n - m] e^{-j\omega n} \quad (6)$$

where  $w$  is the window function,  $x$  is the discrete time series,  $m$  is discrete, and  $X$  is calculated FT.

As shown by fig. 4, the maximum power and angular velocity occurred at the end of data collection from about 670 s until 850 s. To investigate tower behavior during this time span, the last section is separated, and then eq. (6) is applied to plot fig. 7. Normalized magnitudes are specified by different colors varying from white to red which represent zero and 1, respectively. Apparently, the 10 Hz frequency was excited during most of the record. This frequency corresponds to second bending mode according to the FEM.

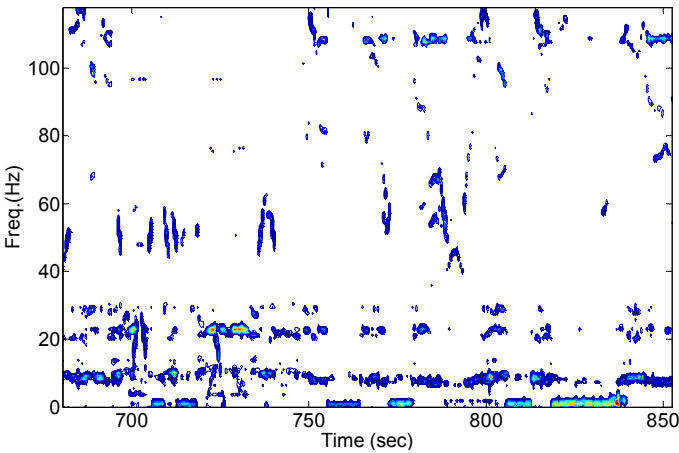


Figure 7: Spectrogram of last section of collected data

There are excitations of 23 Hz corresponding to the fourth bending mode. This frequency has its highest peaks around 722 sec and 730 sec. During this period, power and angular velocity are roughly constant. The frequency band of 40-60 Hz shows many peaks which were excited. These peaks are almost vertical lines in fig. 7. This behavior implies forced frequency at this band. Besides, it is shown that natural frequency of 45 Hz was excited once during this section of data acquisition at around 790 sec. This illustrates why it had a small magnitude in fig. 5. It is also true about two last resonances (85 and 94 Hz). Another significant result from fig. 7 is that some clusters happened at very low frequency below 2 Hz corresponds to the first fundamental bending mode. These high amplitude peaks, especially the last one, only happened at specific times. To study these regions, output power and RPM logs are zoomed in and then were decomposed as indicated by fig. 8. The lengths of the designated selected regions are shown by black lines.

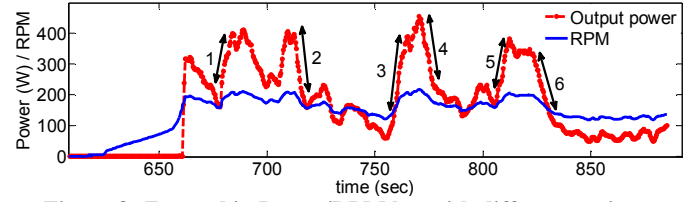


Figure 8: Zoomed in Power/RPM log with different regions

Regions 1, 3, and 5 have rotor acceleration and increasing power whereas 2, 4, and 6 display the converse behavior. The corresponding time periods are given in Table 2.

No.	Time period (sec)		Blades freq. (Hz)	No.	Time period (sec)		Blades freq. (Hz)
	Start	End			Start	End	
1	705	709	8.75-10.5	4	771	777	8.75-10.8
2	712	718	7.75-10.4	5	805	812	7.9-10.7
3	755	764	6.1-10.25	6	823	839	7.0-9.8

Table 2: Different regions specifications according to Fig 8

Figure 9 shows when wind speed and output power increase (or decreases), the first natural frequency which is the fundamental bending mode in both directions (two orthogonal sides) will be excited.

When the blades encounter the tower, it would produce noise and extra excitations. Equation (6) gives the blades passing frequency ( $f_{blades}$ ) and its harmonics ( $f_H$ ).

$$f_{blades} = N f_R, \text{ and } f_H = n f_{blades} \quad (6)$$

where  $N$  is number of blades, and  $f_R$  is rotor frequency. Considering that blades rotational speed reached at 250 r.p.m. at the most, the frequency range up to 12.5 Hz might be potentially contaminated by this effect.

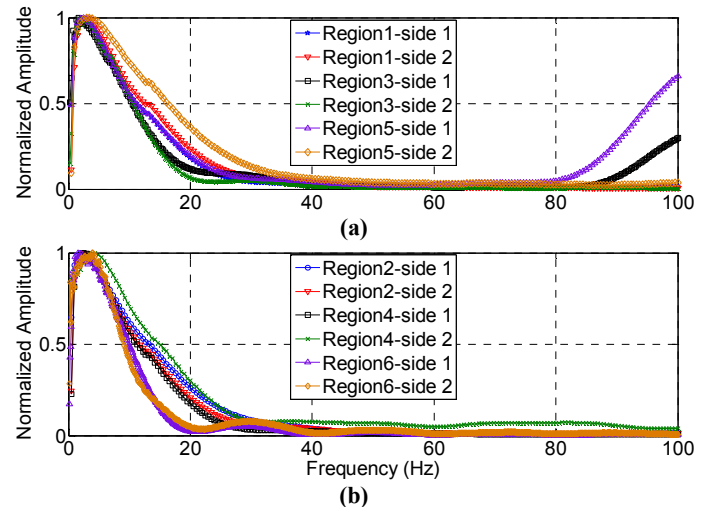


Figure 9: Frequency response when (a) power increases (b) decreases

Those peaks in fig. 9, however, are not as a result of blades passing as according to Table 2, blades frequency ranges in

those regions are much higher changing from 6 to 11 Hz. This means blade passing excited the second natural frequency when  $f_{blades} \cong 10 \text{ Hz}$ . It is illustrated in fig. 7 by several small dots at 10 Hz in the mentioned regions. It seems that wind speed and angular velocity increases lead to excitation of the first bending mode. This is consistent with the analysis of the previous section, where it was found that most vibration energy is in the range of 0-20 Hz.

When there are different regimes of wind speeds and output powers, switching from accelerating blade speed to deceleration excite all other modes as it contains much more impulsive contents. These contents could excite the wide range of frequencies in which natural frequencies are placed.

### ENERGY DISTRIBUTION

From the previous section, it was clear that the dominant peaks occur at lower frequency bands. However, those peaks are not essentially indicative of noise emission at lower frequencies. To determine how vibration energies are distributed along different frequency bands, one can use discrete wavelet decomposition. Its complete theory and further explanations are discussed in many texts on signal processing such as [13,14]. On the whole, two sets of high pass and low pass filters are used at any stage to divide the incoming signal into ‘‘Approximations’’ ( $A$ ) and ‘‘Details’’ ( $D$ ).  $A$  are output of the low-pass filter, while the outputs from the high-pass filters represent  $D$ . The detail portion is saved whereas one may process the  $A$  by using another low- and high-pass filter to take new  $A$  and  $D$ . This decomposition procedure may be done until to capture desirable smallest frequency band. Therefore, the time series ( $\alpha$ ) is sum of this decomposed frequency bands:

$$\alpha = A^7 \sqcup D^7 \sqcup D^6 \sqcup D^5 \sqcup D^4 \sqcup D^3 \sqcup D^2 \sqcup D^1 \quad (7)$$

where  $A$  and  $D$ s represent decomposed signals at different frequency band.  $\sqcup$  indicates union, and the superscript refers to the level. A 7-level decomposition using Daubechies wavelet of order 8 was performed. The smallest band is 0-9.76 Hz. Note again that in each level of decomposition, size of decomposed series is half the previous level.

As the signal energy is proportional to the squared magnitude, then, Root Mean Square (RMS) values for different bands will be calculated according to eq. (8). For  $n$  values of  $x$  the RMS value is

$$RMS = \sqrt{\frac{1}{n} \sum_{i=1}^n (x_i - \bar{x})^2} \quad (8)$$

where  $\bar{x}$  is the mean amplitude of the signal. However, it is mentioned in [15] that vibration signal energies are dependent on different factors such as damping, stiffness properties, atmospheric disturbances, and etc. As a result, RMS itself would not be a good indication of energy distribution and

instead, normalized RMS which is defined by eq. (9) would result in a better indication.

$$RMS_i = \frac{\sqrt{\frac{1}{n_i} \sum_{j=1}^{n_i} (x_j^i - \bar{x}^i)^2}}{RMS_{total}} \quad (9)$$

where  $i$  is number of decomposition levels in the wavelet analysis which is 7 in our case, and  $RMS_{total}$  corresponds to the RMS value of the original time signal.

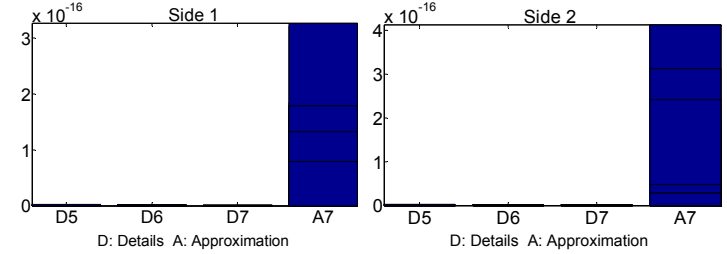


Figure 10: RMS values for different frequency bands

Figure 10 illustrates the relative RMS values for all channels in different frequency bands where  $D_i$ : Details coefficients at different levels, and  $A_7$ : Approximation coefficient at level 7. listed in Table 3.

	A7	D7	D6	D5	D4	D3	D2	D1
Freq	0-10	10-20	20-40	40-78	78-156	156-312	312-625	625-1250

Table 3: Frequency bands using DWT

Although the time series were not decomposed by the same length, it can be seen that most of vibration energy is absorbed in the lowest frequency band which is about 0-10 Hz. In other words the smallest frequency band has the smallest time length as well, however it contains higher energy. This range of frequency, as explained previously, covers the infrasound region that might be perceived at sufficiently high sound pressure level, and acoustic tests would not be good way to show it.

### CONCLUSION

This paper investigated the vibration of a small wind turbine tower. Mechanical noise generated by the turbine would be amplified by its tower as a line source of noise. Natural frequencies and corresponding deflection shapes were compared to the results of a finite element model with the turbine mass and centre of mass included. If the turbine is not operating and the only input force is wind, then only first two modes resonate significantly. It was discovered that first three bending modes are excited more often than others during operation, which could produce most of the noise propagation. Moreover, it was revealed that while blade speed varied continuously along with the power, only the first fundamental bending mode which is about 1.3 Hz, was excited. Thus the first bending mode plays a crucial role in generating vibration

and noise. As a general rule of thumb, most of vibration energy is thought to be engaged in very low frequency bands.

## ACKNOWLEDGMENTS

The authors would like to thank the ENMAX Corporation., and the Natural Sciences and Engineering Research Council (NSERC) of Canada for financial support under the Industrial Research Chair program. Colin Dumais, the owner of the turbine, provided much support that is gratefully appreciated. Also, the authors express gratitude to David Ford and Jayson Russell who modeled the FEM.

## REFERENCES

- [1] Sorensen, J. D. and Sorensen, J. N., 2011, "Wind Energy Systems, Optimising design and construction for safe and reliable operation", Woodhead Publishing Series in Energy.
- [2] Migliore, P., van Dam, J. and Huskey, A. "Acoustic tests of small wind turbines" AIAA-2004-1185.
- [3] Rogers, A. L. and Manwell, J. F., 2002, "Wind Turbine Noise Issues", Renewable Energy Research Lab, University of Massachusetts at Amherst.
- [4] Marmo, B. A. and Carruthers, B. J., "Modeling and Analysis of Acoustic Emissions and Structural Vibration in a Wind Turbine", COMSOL Conference, Paris, 2010.
- [5] Fan, S., Min, Z. and Chen, H. "Modal identification from output-only in frequency-domain", Proc. 5<sup>th</sup> Int. Conference on Vibration Engineering, 2002.
- [6] Brincker, R., Zhang, L. and Andersen, P., 2000, "Modal Identification from Ambient Responses using Frequency Domain Decomposition", Proc. of the 18<sup>th</sup> International Modal Analysis Conference, San Antonio, TX.
- [7] Bao, Z. W. and Ko, J. M., 1991, "Determination of modal parameters of tall buildings with ambient vibration measurements", Int. Journal of Analytical and Experimental Model Analysis, **6**, pp. 57-68.
- [8] Larbi, N. and Lardies, J., 2000, "Experimental modal analysis of a structure excited by a random force", Mechanical Systems and Signal Processing, **14**, pp. 181-192.
- [9] James, G. H. and Carne, T. G., 1995, "The natural excitation technique (NExT) for modal parameters extraction from operating structures", Modal Analysis, **10**, pp.260-277.
- [10] Brincker, R., Andersen, P., and Moller, N., 2000, "Output-Only Modal Testing of a Car Body Subject to Engine Excitation", Proc. of the 18<sup>th</sup> Int. Modal Analysis Conference, San Antonio, TX.
- [11] Shen, F., Zheng, M., Feng Shi, D. and Xu, F., 2002, "Using the cross-correlation technique to extract modal parameters on response-only data", Journal of Sound and Vibration, **259**, pp.1163-1179.
- [12] Herlufsen, H. and Moller, N., 2002, "Operational Modal Analysis of a Wind Turbine Wing Using Acoustical Excitation", Bruel & Kjar Application Note.
- [13] Chui, C. K., 1992, "An Introduction to Wavelets", Academic Press, New York, pp. 1-200.
- [14] Daubechies, I., 1990, "The wavelet transform, time-frequency localization and signal analysis", IEEE Transactions on Information Theory, **36**, pp.961-1005.
- [15] Sun, Q., Tang, Y., Yang Lu, W. and Ji, Y., 2005, "Feature Extraction with Discrete Wavelet Transform for Drill Wear Monitoring", Journal of Vibration and Control, **11(11)**, pp.1375-1396.